Reconnaissance of Infrared Emission from the Lunar Nighttime Surface[1]

ROBERT L. WILDEY[2]

Division of Geological Sciences, California Institute of Technology and Mount Wilson and Palomar Observatories Pasadena, California 91109

BRUCE C. MURRAY AND JAMES A. WESTPHAL

Division of Geological Sciences, California Institute of Technology Pasadena, California 91109

Introduction. The reconnaissance described in this paper was performed in 1964 and is an extension and refinement of the first observations (1962), in the 8- to 14-μ wavelength region, of the thermal emission from the lunar nighttime surface [*Murray and Wildey,* 1964]. The present investigation was intended to sample representatively enough of the lunar surface to determine the general character of the lunar nighttime emission and the relative abundance of nighttime infrared anomalies.

More complete studies of the infrared emission with higher spatial resolution during *eclipse* were made at about the same time [*Saari and Shorthill,* 1965].

These two kinds of infrared observations are complimentary since the nighttime emission reflects thermal properties at centimeter depth, in granular material, whereas the eclipse emission is influenced mainly by the uppermost millimeter of such material. Also, the effects of varying albedo can be ignored in the interpretation of the nighttime data.

In the present paper, the observations will be presented with only a minimum of interpretation. Some interpretative questions have been discussed briefly elsewhere [*Murray,* 1965*a, b*] or are in preparation [*Wildey,* 1967]. Comprehensive geophysical analysis of lunar structure requires, however, an integrated interpretation of infrared data in conjunction with polarization data, radar data, radio data, photoelectric photometry and colorimetry, and high-resolution photography such as that being acquired by Lunar Orbiter.

Observational procedure. The 8- to 14-μ photometry was carried out with the 24-inch telescope and photometer arrangement also used in the investigation reported by *Becklin and Westphal* [1966], except that the telescope was located at 10,500 feet on White Mountain, near Bishop, California. Observations were collected during parts of the lunations of July and August 1964, but, owing to mechanical problems and weather, only the nights of August 28, 29, and 30 yielded observations of sufficient quality and coverage to permit cataloging of anomalies. Only on August 29 were conditions sufficiently favorable to permit infrared mapping of the nighttime lunar surface. The relevant physical information on the anomalies is summarized in Table 1. The intensity calibration was obtained by observing Jupiter through an air mass similar to that through which the moon was observed. A peak brightness temperature of 129°K has been assumed for Jupiter [*Wildey et al.,* 1965]. It is estimated that maximum systematic errors in the absolute calibration are less than 25% in specific intensity. The minimum detectable surface brightness corresponds to that of a 100°K blackbody above the atmosphere; however, temporal fluctuations in the balance of the two beams of the photometer, usually due to the effects of wind on the telescope tube, introduced perturbations in the zero reference of the scans, in some instances. This effect is, in fact, the principal reason mapping could only be accomplished on a single night.

The diaphragm was 1.22 mm in diameter, re-

[1] Contribution 1442 of the Division of Geological Sciences, California Institute of Technology, Pasadena.

[2] Now at Center of Astrogeology, U. S. Geological Survey, Flagstaff, Arizona 86001.

TABLE 1. Catalog of Lunar Nighttime Anomalies

I is defined as a true thermal surface brightness. It is termed specific intensity in the theory of stellar atmospheres, and elsewhere it is often called luminance. Its absolute units are watts/cm²/steradian/$\Delta\lambda$, and it is directly proportional to the photometer signal in the case of an extended object. The unit of ΔI used in column four is the thermal brightness of a water-ice blackbody. In column three $\Delta I/I$ is the ratio of the peak brightness (hence signal) *excess* of an anomaly to the brightness (or signal) of the surrounding region.

Location		Description				Remarks
		W/R*	$\Delta I/I$†	$\Delta I(10^{-4})$‡	$\lambda - \lambda_t$§	
26E36S	Crater Rabbi Levi	1.0	0.10	6.2	4.3	Highland
29E35S	In or near Crater Riccius	1.0	0.10	5.2	7.3	Highland
34E33S	Crater Stibborius	1.0	0.15	7.1	34.7	Highland
32E32S	Crater Stibborius–Crater Piccolomini	2.0	0.50	17.0	3.3	Highland
25E31S	Crater Lindenau	1.0	0.20	17.0	3.3	Highland
27E28S	Altai Scarp	1.0	0.90	15.0	29.7	Highland–mare boundary
46E27S	In or near Crater Borda	2.0	1.00	11.0	44.3	Highland
52E25S	In or south of Crater Borda	1.0	1.00	16.0	30.3	Edge of Mare Fecunditatis
58E29S	Crater Snellius	1.5	1.60	11.0	60.7	Highland
65E33S	Between Crater Adams and Crater Furnerius	1.5	0.80	6.0	55.5	Highland
02E24S	Crater Lacaille	1.0	0.17	13.0	4.7	Highland
14E17S	Edge of Crater Almanon	2.0	0.20	6.8	16.7	Highland
15E16S	Crater Almanon	1.0	1.00	60.0	5.5	Highland
16E22S	Near Crater Sacrobosco	1.0	0.20	6.4	18.7	Highland
26E16S	Crater southeast of Crater Cyrillus	1.5	0.10	6.6	4.3	Highland near Mare Nectaris
35E14S	Middle of Mare Nectaris	1.5	0.80	10.0	37.7	Near small bright crater
39E14S	West of Pyrenees on edge of Mare Nectaris	1.0	0.45	16.0	17.3	Small crater
46E12S	East of Crater Santbech	1.0	1.00	24.0	24.3	Mare
49E11S	4° east of Crater Goelenius	1.0	0.80	10.0	39.5	Mare
53E12S	In Mare Fecunditatis	2.0	3.50	28.0	55.7	Mare
50E17S		2.0	0.70	8.0	40.5	Highland
59E15S	West rim of Crater Vendelinus	1–1.5	2.00	15.0	61.7	Highland–mare boundary
60E17S	West rim of Crater Vendelinus	1.0	2.00	25.0	38.3	Mare?
02W08S	Inside Crater Ptolemaeus	1.0	0.24	21.0	0.7	Includes halo crater
11E07S		1.0	0.15	6.1	13.7	Highland
15E10S	Crater Dolland	1.0	0.11	6.8	5.5	Highland
13E03S		1.0	0.10	6.9	3.5	Highland
25E04S	Near Crater Hypatia	1.0	0.10	7.1	3.3	Highland–mare boundary
28E09S	Near or on rim of Crater Theophilus	1.0	0.10	6.0	6.3	Between Mare Tranquillitatis and Mare Nectaris
32E04N	Near Crater Maskelyne	1.5	0.20	6.0	22.5	Highland–mare boundary
30E03S	Between Crater Censorinus A and Crater Torricelli	1.0	1.00	15.0	32.7	Mare
30E00S	Mare Tranquillitatis	1.0	1.00	15.0	32.7	Mare
34E02S	Near Crater Censorinus A	1.0	0.10	4.3	12.3	Highland
36E01N	Mare Tranquillitatis	4.0	0.60	13.0	26.5	Mare
43E01N	Near Crater Secchi	1.0	0.20	6.0	21.3	Highland–mare boundary
49E05S	Mare Fecunditatis	2.5	0.20	2.8	27.3	Mare
62E09S	Crater Langrenus	1.0	0.60	5.8	52.5	Central peak?
62E08S	Crater Langrenus	1.0	0.40	5.8	52.5	Highland–mare boundary
64E04S	2° northeast of Crater Lohse	1.2	2.20	14.0	66.7	Highland

TABLE 1. (Continued)

	Location	Description				Remarks
		W/R*	$\Delta I/I$†	$\Delta I(10^{-4})$‡	$\lambda - \lambda_i$§	
10E03N	Near Craters Godin and Agrippa	1.0	0.15	6.5	12.7	Highland
07E08N	Near Crater Hyginus and Hyginus Rille	1.5	0.20	10.0	9.7	Mare
17E03N	Near or on Crater Dionysius	1.0	0.10	5.6	7.5	Mare
17E02N	Southwest of Crater Dionysius	1.0	0.60	34.0	7.5	Highlands
19E06N	Near Craters Manners and Arago	1.0	0.30	15.0	9.5	Mare
19E05N	Near Crater Manners	1.0	0.50	15.0	21.7	Mare
22E06N	Crater Arago	1.0	0.07	7.0	0.3	Mare
17E08N	Near Craters Sosigenes and Julius Caesar	1.0	0.28	16.0	7.5	
21E10N	South of Crater Ross	4.0	0.80	21.0	23.7	Mare
24E07N	Mare Tranquillitatis	1.0	0.10	7.7	2.3	Mare
25E07N	Mare Tranquillitatis	2.0	0.10	3.8	15.5	Mare
27E07N	Mare Tranquillitatis	2.0	0.20	3.6	29.7	Mare
23E03N	Mare Tranquillitatis	2.0	0.20	8.2	13.5	Mare
31E09N	Near Crater Sinas	1.0	0.15	7.5	9.3	Mare
35E10N		2.5	0.10	4.3	13.3	Mare
33E08N		1.0	0.20	5.6	23.5	Mare
51E02N		1.0	0.50	9.0	29.3	Mare
02W18N	Appenine Mountains	1.0	0.35	35.0	0.7	
21E15N	Near Crater Plinus	1.0	0.18	8.3	11.5	
26E10N	Mare Tranquillitatis	3.0	0.80	30.0	16.5	Highland–mare boundary
27E16N	In Mare Tranquillitatis 3° from Craters Plinius and Dawes	1.5	1.0	36.0	17.5	Mare
35E17N	In Mare Tranquillitatis	1.0	0.5	12.0	25.5	Small highland peninsula
40E13N	Between Palus Somni and Mare Tranquillitatis	1.0	1.80	22.0	42.7	West edge of highland
42E18N	Dark‖ area northwest of mouth of Pallus Somni	1.0	0.70	16.0	32.5	Marginal, mare
57E13N	All of Mare Crisium	2.0	0.50	6.5	35.3	Mare, broad anomaly
71E14N	Crater Hansen	1.4	0.30	2.9	49.3	Highland
04E27N	Mt. Hadley, near Mare Serenitatis	1.5	0.11	6.2	6.7	Highland
08E23N	In Mare Serenitatus near bright‖ spot	1.0	0.23	11.0	10.7	Mare
10E19N	High ridge in Haemus Mountains, 2° west of Sulpicius Gallus	1.0	0.35	+ 35.0	0.5	Highland near mare or vice versa
17E21N	In Mare Serenitatis 2° west of Crater Bessel	1.0	0.80	43.0	7.5	
20E20N	In Mare Serenitatis 2° west of Crater Deseilligny	5.0	0.70	20.0	22.7	Mare, broad but marginal anomaly
22E19N	In Mare Serenitatis	1.0	0.35	8.8	24.7	Mare, featureless region
11E28N	In Mare Serenitatis 2° northwest of bright spot Linne	1.0	0.38	16.0	13.7	Mare
18E27N	In Mare Serenitatis 1.5° east of bright halo crater	1.0	0.10	5.0	8.5	Mare
25E30N	In Mare Serenitatis 6.5° southwest of Crater Posidonius	2.0	0.60	12.0	27.7	Mare, bright spot end of sinuous rille
25E28N	Sinuous rille in Mare Serenitatis	1.0	0.30	12.0	15.5	Mare
23E25N	In Mare Serenitatis 1.5° east of bright spot halo crater	1.0	1.40	34.0	25.7	Mare
26E22N	Sinuous rille in Mare Serenitatis	1.0	0.10	6.7	4.3	Mare
25E22N	Sinuous rille in Mare Serenitatis	3.5	0.30	12.0	15.5	
23E23N	Very small bright halo crater in Mare Serenitatis	1.0	2.25	52.0	25.7	

TABLE 1. (Continued)

Location		Description				Remarks
		W/R*	$\Delta I/I$†	$\Delta I(10^{-4})$‡	$\lambda - \lambda_t$§	
29E23N	Crater ray southeast LeMonnier's archipelago	1.5	0.05	2.8	7.3	Mare (Serenitatis)
31E25N	Upland mountains southeast of Le Monnier	1.5	1.00	13.0	33.7	Highland
35E24N	In rugged uplands, features indistinct	1.0	0.4	17.0	13.3	Highland
44E26N	Dark region in uplands	2.0	0.2	5.8	22.3	Highland
11E34N	Tiny bright halo crater in Mare Serenitatis	1.0	0.08	6.8	1.5	Mare
18E31N	In field of small bright halo craters in Mare Serenitatis	1.0	0.1	···	−3.7	Mare
21E32N	In field of small bright halo craters in Mare Serenitatis	1.0	0.35	35.0	−0.7	Mare
26E32N	In Mare Serenitatis	1.4	0.30	20.0	4.3	Mare
25E36N	In Lacus Somniorum	1.0	0.20	7.6	15.5	Mare, not reproduced
24E33N	Crater Luther in Mare Serenitatis	1.0	0.25	6.0	26.7	Mare, marginal case
28E34N	Larger bright halo crater between Luther and Posidonius	1.0	0.50	8.5	30.7	Mare
29E33N	Among 3 bright halo craters in Mare Serenitatis	1.0	0.25	13.0	7.3	Mare
36E37N	Among bright spots in Lacus Somniorum	2.0	0.15	5.5	16.5	Mare
41E32N	Rugged uplands, rim of Serenitatis basin	1.0	1.00	11.0	43.7	Highland
03E45N	Old crater in uplands between Mare Frigorus and Mare Imbrium	1.0	1.00	60.0	5.7	Highland
29E47N	1° north of large Crater Burg in Lacus Martis	1.2	0.45	25.0	7.3	Mare
28E44N	Crater Burg	1.5	0.40	13.0	18.5	Mare, not reproduced
33E48N	Crater Baily	1.0	0.25	11.0	11.3	Unusual mare
38E53N	Upland isthmus between Mare Frigors and maria-filled Crater Endymion	2.0	0.50	17.0	18.5	Highland
39E49N	3° north of Crater Hercules	1.3	0.40	14.0	17.3	Highland
42E47N	Near rim of Crater Atlas	1.0	0.70	10.0	32.5	Highland, not reproduced
37E45N	West rim of Hercules	1.2	2.80	40.0	32.7	Highland
10E53N	In Mare Frigoris 1° from bright halo crater	1–2	1.20	52.0	12.7	Mare
13E54N	In Mare Frigoris	1.0	0.10	···	−8.3	Mare, tall mountain peak
04E58N	In Mare Frigoris 2° southwest of Crater Archytas	1.0	0.20	···	−17.3	Mare
22E57N	In Mare Frigoris 1° north of Crater Galle	1.0	0.10	10.0	0.3	Mare
37E59N	Uplands east of Mare Frigoris	2.0	0.30	12.0	15.3	Highland, superposition confused
19E51N	East rim of Aristoteles	2.0	0.70	35.0	9.5	Mare
27E55N	In Mare Frigoris near Crater Galle	1.6	0.50	9.0	29.7	Mare, marginally reproduced
54E51N	In crater chain 2° south of Crater Endymion	1.0	0.35	5.5	32.3	Highland
53E64N	North of Crater Strabo	1.0	2.20	17.0	55.7	Highland

* The apparent width of the anomalous feature expressed as a ratio to the instrumental spatial resolution.
† The relative intensity contrast of the anomaly to the surrounding area.
‡ The peak intensity from the anomaly expressed as a fraction of the brightness from a 273° K blackbody.
§ The longitude difference between the anomaly and the terminator at the time of the observation.
‖ Visible light.

sponding to an area 45 ± 2 km in diameter at the subearth point of the moon (1/77 of the lunar diameter). Expressed in degrees of lunar latitude at the subearth point, this corresponds to a circle of 0.7° radius. The spatial resolution of the photometer is estimated to be approximately that defined by the geometric aperture.

The telescope was set to track the moon in declination, and drift curves were made in pairs. Each pair was offset approximately 1.5 arc minute of declination. Multiple photographs of the lunar image reflected from the aperture plate were acquired through the photometer during each scan after passage onto the bright side of the moon. Hence, transcription to an appropriately librated selenographic coordinate projection could be made both directly from the photographs and from ephemeris data and the time of terminator crossing, which was also recorded. Both methods were used and compared; a maximum absolute positional error corresponding to three times the aperture dimension has been estimated on this basis. A more elaborate positioning technique [*Wildey*, 1964] designed for this work was not used owing to a lack of proper data handling facilities.

Data. Figure 1 is an 8- to 14-μ brightness temperature map of the nighttime surface of the moon acquired on the night of August 29, 1964. The terminator position shown is as it appeared visually and photographically through the photometer. The unexpectedly complex brightness temperature distribution arises from the large number of nighttime thermal anomalies and from irregular enhancements of some maria regions.

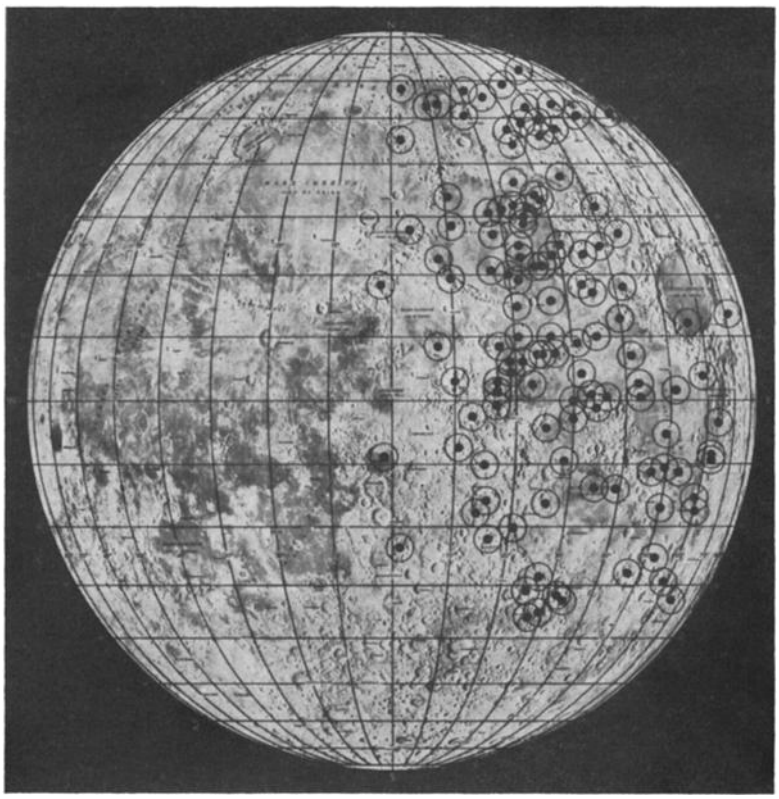

Fig. 1. Location of nighttime infrared anomalies observed on the nights of August 28, 29, and 30, 1964. Filled circles correspond to aperture size and surrounding circles define maximum positional uncertainty. Base map is mosaic compiled by the U. S. Air Force Aeronautical Chart and Information Center, (LEM-1A, 2nd Edition, November 1962).

Table 1 is a catalog of nearly all anomalous infrared emission features recognizable on the scans of the three nights August 28, 29, and 30. Figure 2 shows the locations of these anomalies on the moon. No areas of anomalously low emission were recognized. Some duplication exists between entries of similar selenographic coordinates acquired on successive nights. Also, true associations of anomalies also exist and individual features occasionally show considerable structure. Associations, duplications, or both are evident from Figure 2 and are indicated by grouped entries in Table 1.

Approximately one-third to three-quarters of the available nighttime surface was sampled on each of the three nights. Noting that the average number of anomalies detected per night is about 35, and that about 50% of the moon was shadowed, one would estimate the total number of such anomalies on the visible hemisphere of the moon to be close to 200.

Interpretation. A most striking feature of Figure 1 is the low level enhanced emission from some maria areas, especially Mare Crisium. Similar but not completely corresponding effects have been observed in the eclipse data [*Saari and Shorthill,* 1965]. In particular, the enhanced emission of Mare Crisium is peculiar to the lunar nighttime. We have investigated whether a systematic difference in thermal properties of maria and upland regions is indicated by the scans acquired on August 29. This was accomplished by comparing portions of the midlatitude scans that are free from strong anomalies,

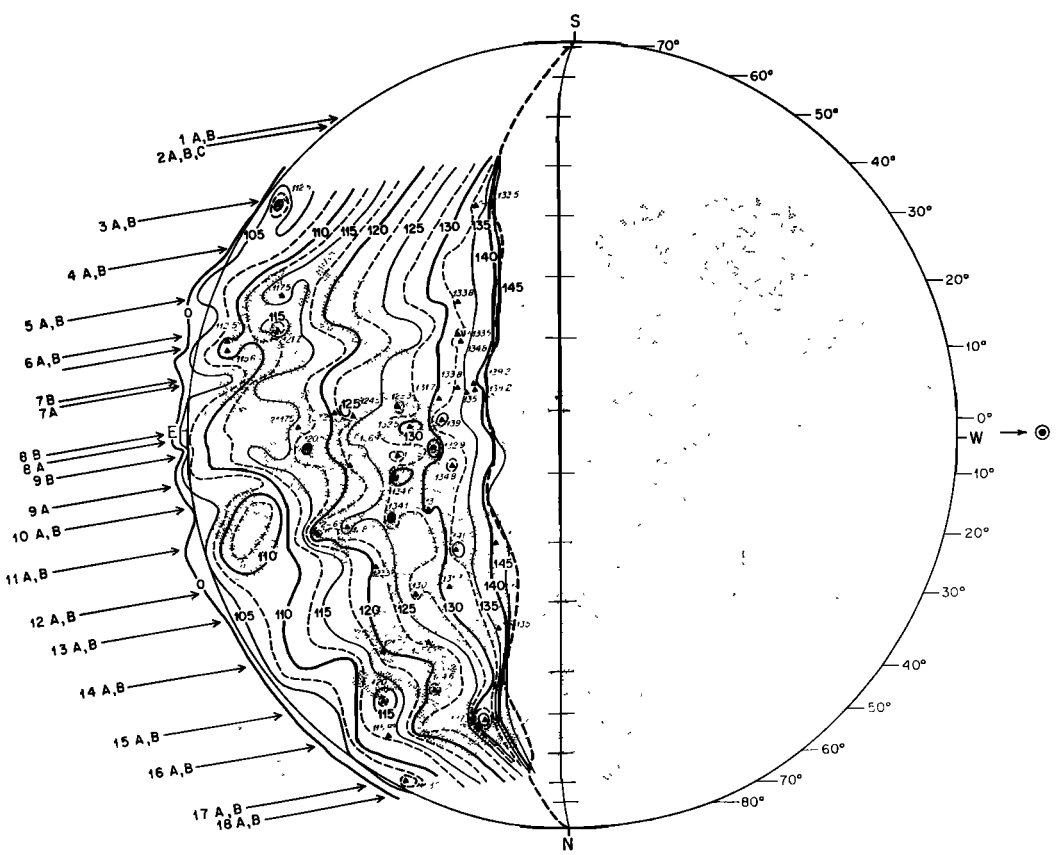

Fig. 2. Brightness temperature (8–14 μ) map for third quarter moon of August 29, 1964, 1030 to 1156 hours UT. Terminator tracing is shown as heavy curve. Small triangles are narrow infrared anomalies or hot spots obtained the same night (see Table 1 for those of all nights). Mare regions are shaded. The librated lunar equator and prime meridian are mapped. Arrows at disk edge indicate scan tracks with numbers and letters for retraces.

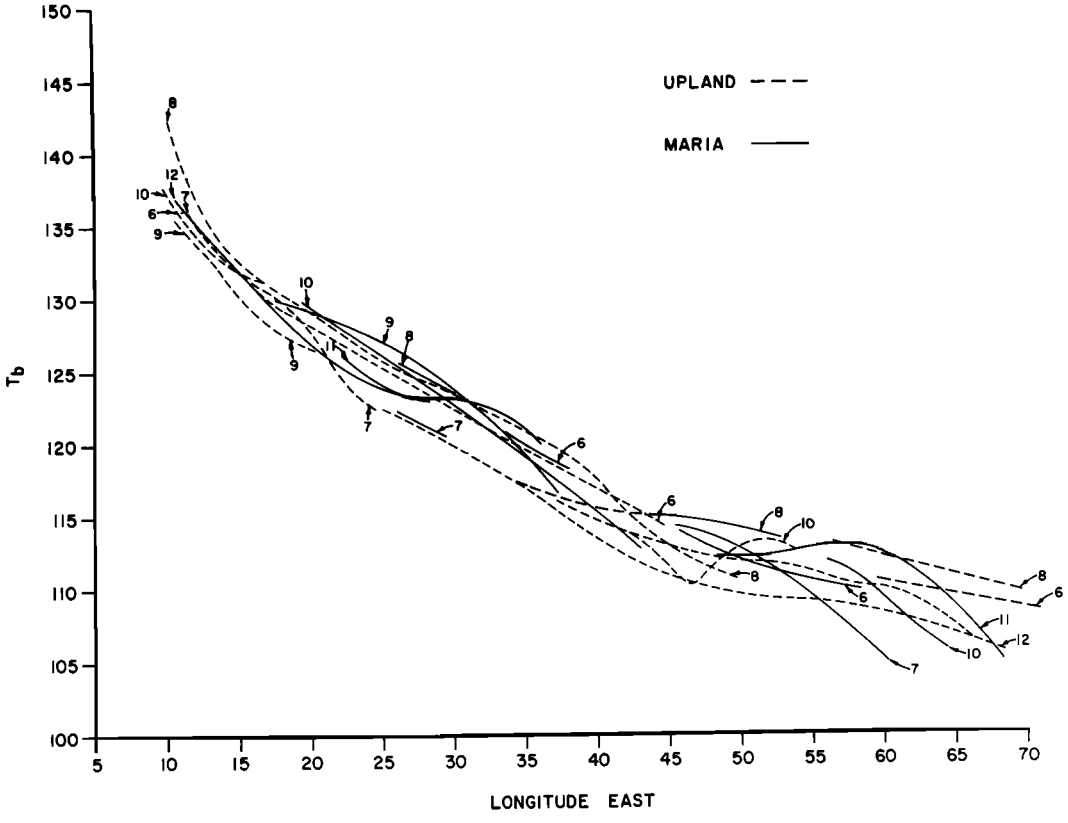

Fig. 3. Brightness temperature versus selenographic longitude for several of the scans of Figure 1. Hence, the normal lunar cooling curve. Note difference curve representation for emission from maria and uplands. Terminator longitude (average) is 9.5°E.

as shown in Figure 3. It can be seen that any systematic difference is concealed by the intrinsic variability of each region. The scatter of Figure 3 can also be taken to represent the level of precision to which 'the' lunation cooling curve of 'the' moon is meaningful.

Acknowledgment. This research was supported by funds of grant NSG 56-60 from the National Aeronautics and Space Administration.

References

Becklin, E. E., and J. A. Westphal, Infrared observations of comet 1965f, *Astrophys. J., 145,* 445–453, 1966.

Murray, B. C., Infrared evidence of differential surface processes on the moon, *Symposium on the Physics of the Moon, London, June 1–4, 1965, Royal Society,* p. 124, 1965a.

Murray, B. C., Current problems in the interpretation of lunar physical observations, *Proc. Caltech-JPL Lunar and Planetary Conf., September 13–18, 1965,* pp. 32–33, 1965b.

Murray, B. C., and R. L. Wildey, Surface temperature variations during the lunar nighttime, *Astrophys. J., 139,* 734–750, 1964.

Saari, J. M., and R. W. Shorthill, Infrared observations of the lunar eclipse of December, 1964, *Nature, 205,* 964–965, 1965.

Wildey, R. L., A computer program for the transformation of lunar observations from celestial to selenographic coordinates, *Icarus, 3,* 136–150, 1964.

Wildey, R. L., The nocturnal heat sources of the surface of the moon, *Monthly Notices Roy. Astron. Soc., 128,* to be published, 1967.

Wildey, R. L., B. C. Murray, and J. A. Westphal, Thermal infrared emission of the Jovian disk, *J. Geophys. Res., 70,* 3711–3719, 1965.

(Received February 13, 1967.)